Journal of Molecular Structure 1321 (2025) 140133

Contents lists available at ScienceDirect

Journal of Molecular Structure

journal homepage: www.elsevier.com/locate/molstr

Synthesis and characterization of $MgFe_2O_4$@SiO_2@CBCE-Pd as a novel, green organometallic catalyst, and study of its catalytic activity for C–C and C–O cross-coupling reactions

Durgesh Singh [a,*], Anjan Kumar [b], Yashwantsinh Jadeja [c], Soumya V Menon [d], Priyanka Singh [e], Safaa Mohammed Ibrahim [f], Manmeet Singh [g], Munther Kadhim Abosaoda [h,i], Salwa Bader AlReshaidan [j], Mohammed A. El-Meligy [k]

[a] Department of Chemistry, School of Chemical Sciences & Technology, Dr. Harisingh Gour Vishwavidyalaya (A Central University), Sagar 470003, India
[b] Department of electronics and communication engineering, GLA University, Mathura 281406, India
[c] Marwadi University Research Center, Department of Chemistry, Faculty of Science, Marwadi University, Rajkot 360003, Gujarat, India
[d] Department of Chemistry and Biochemistry, School of Sciences JAIN (Deemed to be University), Bangalore, Karnataka, India
[e] NIMS School of Allied Sciences and Technology, NIMS University, Rajasthan, Jaipur, 303121, India
[f] Department of Optics Techniques, health and medical techniques college, Alnoor University, Mosul, Iraq
[g] Department of Applied Sciences, Chandigarh Engineering College, Chandigarh Group of Colleges-Jhanjeri, Mohali 140307, Punjab, India
[h] College of pharmacy, the Islamic University, Najaf, Iraq
[i] College of pharmacy, the Islamic University of Al Diwaniyah, Al Diwaniyah, Iraq
[j] Faculty of Science, King Saud University, P.O. Box 800, Riyadh 11451, Saudi Arabia
[k] Jadara University Research Center, Jadara University, Jordan Applied Science Research Center, Applied Science Private University, Amman, Jordan MEU Research Unit, Middle East University, Amman 11831, Jordan

ARTICLE INFO

Keywords:
Green
Coupling
$MgFe_2O_4$
Nanoparticles
Catalyst

ABSTRACT

In this work, a new palladium nanocatalyst was supported on CBCE functionalized MNPs ($MgFe_2O_4$@SiO_2@CBCE-Pd) and was characterized by EDS, FTIR, SEM, ICP, XRD, VSM, and TGA techniques. The performance of $MgFe_2O_4$@SiO_2@CBCE-Pd was found to exhibit excellent catalytic activity for C—O and C–C cross-coupling reactions. The nanocatalyst showed high activity and efficiency as evidenced by the excellent yields of products obtained from the C–O and C—C coupling reaction. Additionally, the synthesized nanocatalyst can be retrieved using a magnet and employed for up to four cycles without diminishing its catalytic effectiveness.

1. Introduction

The application of palladium in homogeneous nanocatalysis has been thoroughly explored in different C—C coupling reactions [1–3]. Homogeneously catalyzed coupling reactions achieve high levels of selectivity and reactivity [4,5]. Homogeneous nanocatalysts are associated with several problems, including difficult transport and recyclability, high cost, and difficulty in isolation [6,7]. The mentioned problems can be overcome by using heterogeneous nanocatalysts. Immobilization of homogeneous nanocatalysts on solid support leads to stability in the reaction environment and their efficient recycling [8–13]. To achieve this goal, various materials have been utilized to produce diverse Pd-catalysts, including metal oxides, ionic liquids, carbon, molecular sieves, boehmite, mesoporous silica, and polymers [14,15]. Developing and researching new and efficient nanomaterials as catalytic support is a big challenge in modern organic synthesis [16,17]. Over the past ten years, MNPs have become popular as widely utilized supports in creating magnetic catalysts because of their simple preparation and operation, effortless recovery by the magnetic field, and large surface area. Magnetic nanoparticles offer the advantage of being easily separated from the reaction mixture using a bar magnet [18,19]. Heterogeneous nanocatalysts such as $MgFe_2O_4$ have garnered significant favor due to their simple synthesis and the ease with which their surface can be modified using a magnet. Different catalysts can be fixed onto $MgFe_2O_4$ nanoparticles, allowing for their retrieval and repeated use over multiple cycles [2,20–22].

Carbon-carbon and Carbon-Oxygen coupling reactions are frequently catalyzed by homogeneous or heterogeneous Pd-complexes,

* Corresponding author.
E-mail address: durgesh.phdchem16@gmail.com (D. Singh).

https://doi.org/10.1016/j.molstruc.2024.140133
Received 24 August 2024; Received in revised form 15 September 2024; Accepted 18 September 2024
Available online 19 September 2024

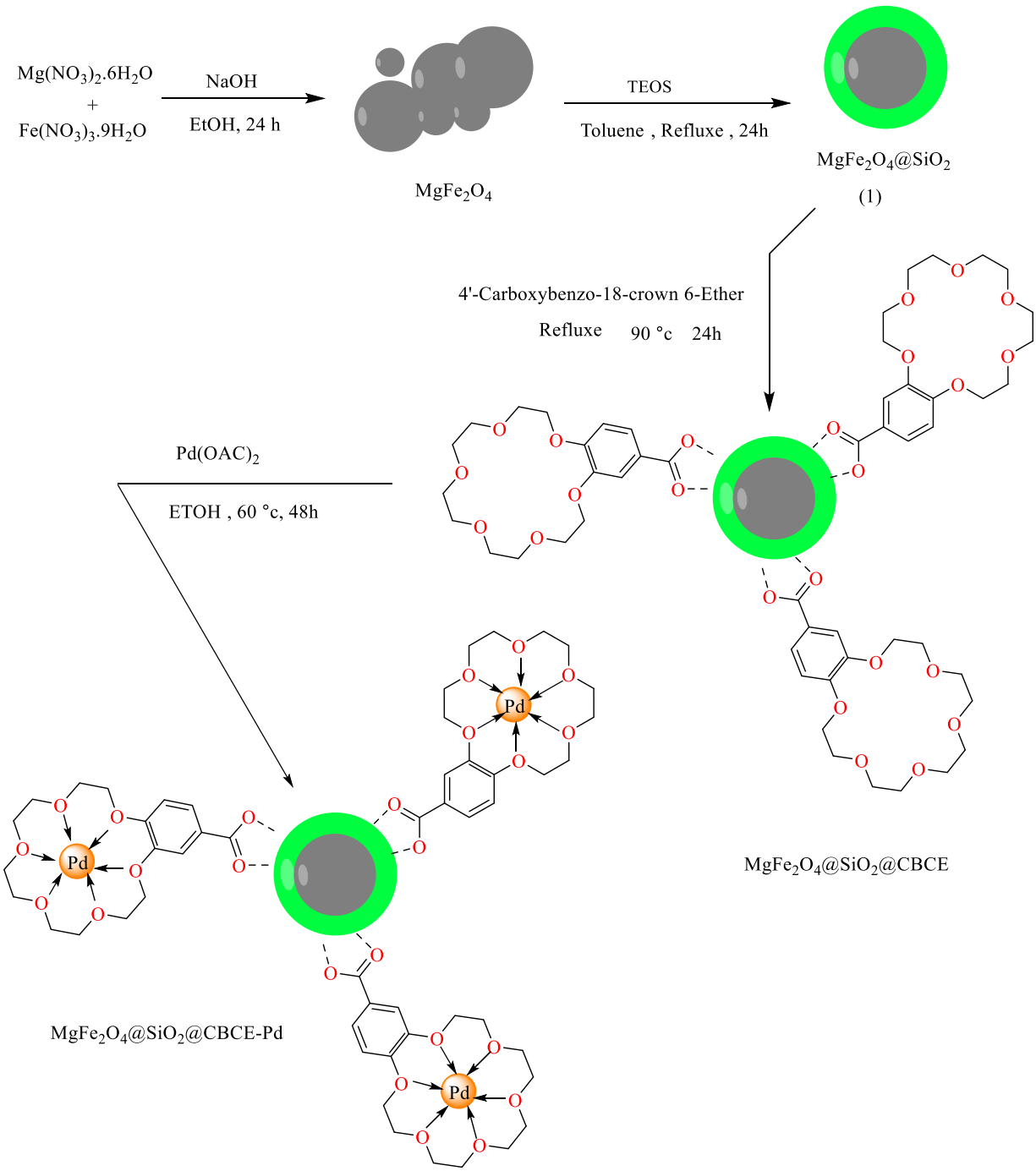

Scheme 1. Synthesis of $MgFe_2O_4$@SiO_2@CBCE-Pd.

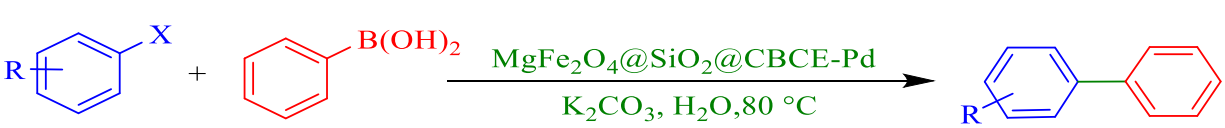

Scheme 2. Suzuki reaction in the presence of $MgFe_2O_4$@SiO_2@CBCE-Pd catalyst.

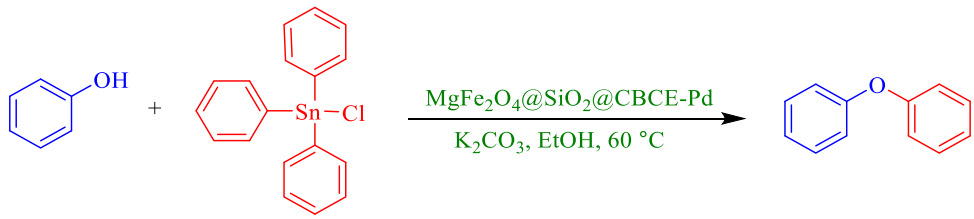

Scheme 3. Synthesis of C–O bond catalyzed by $MgFe_2O_4$@SiO_2@CBCE-Pd.

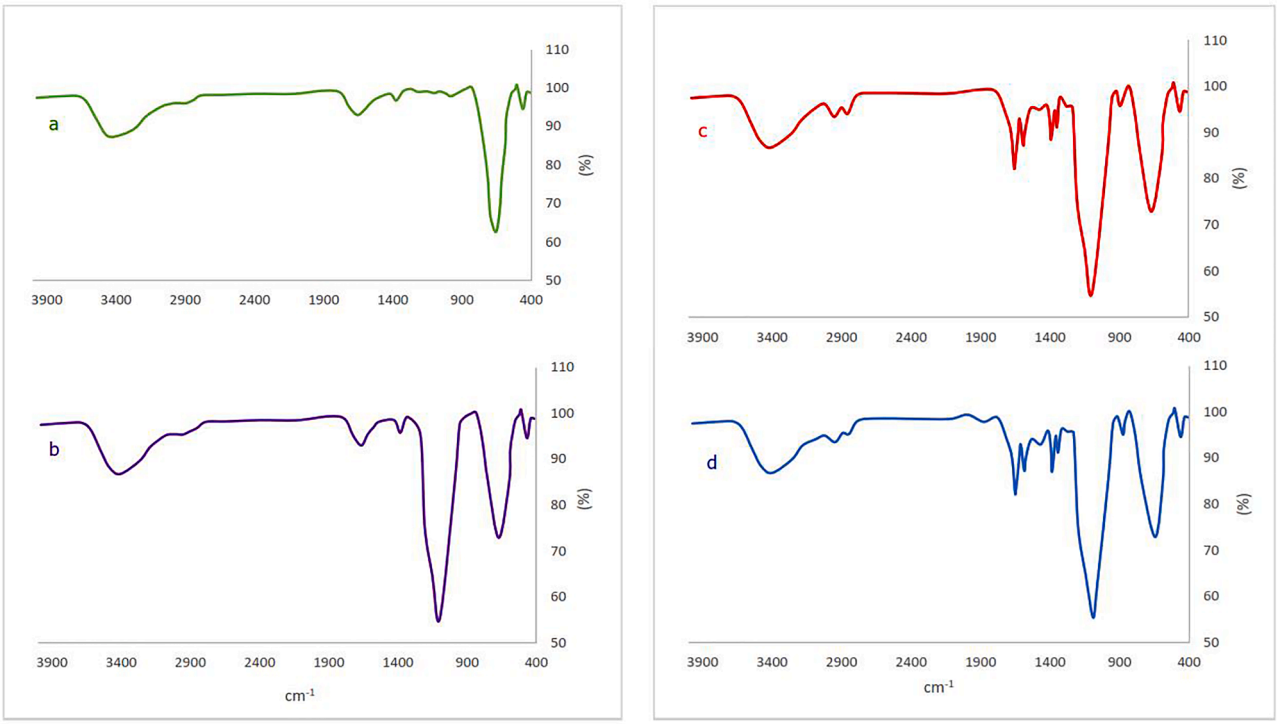

Fig. 1. Comparative study of FTIR spectra of a) $MgFe_2O_4$, b) $MgFe_2O_4$@SiO_2, c) $MgFe_2O_4$@SiO_2@CBCE, d) $MgFe_2O_4$@SiO_2@CBCE-Pd.

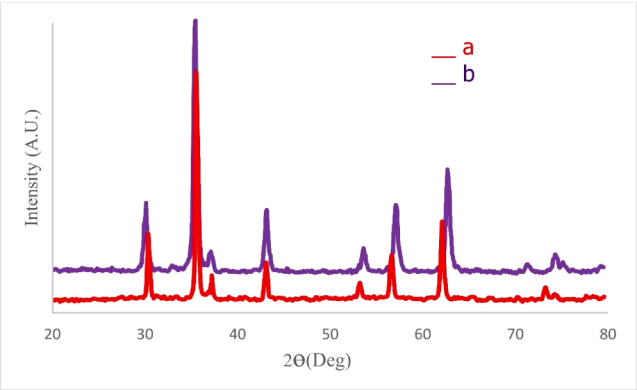

Fig. 2. XRD spectrum of $MgFe_2O_4$@SiO_2@CBCE-Pd (a) and recovered catalyst (b).

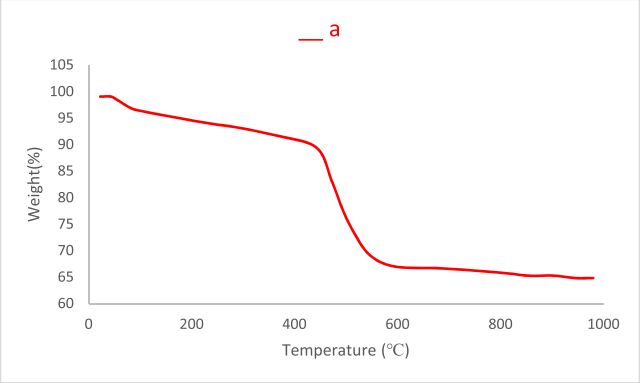

Fig. 3. TGA curve of $MgFe_2O_4$@SiO_2@CBCE-Pd.

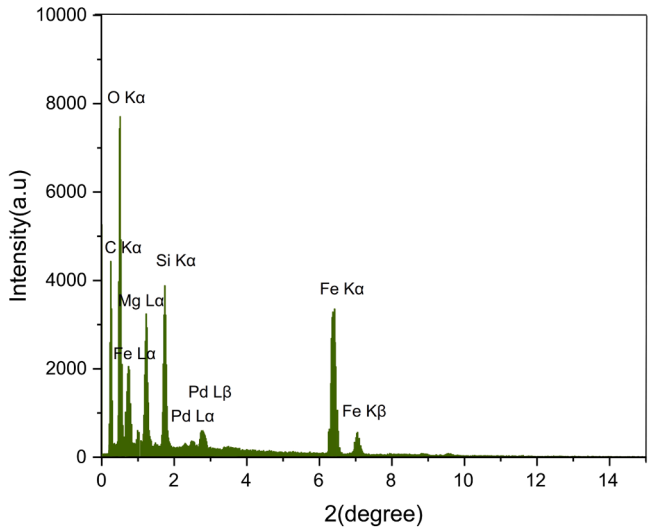

Fig. 4. EDS analysis of $MgFe_2O_4$@SiO_2@CBCE-Pd.

serving as a powerful tool in contemporary synthetic organic chemistry for the synthesis of advanced materials, natural products, UV screens, pharmaceuticals, herbicides, liquid crystal materials, and biologically active compounds [23–26].

In this paper, we present the creation and structural analysis of a new environmentally friendly catalyst designed to stabilize palladium ions. We also explore its effectiveness as a green and efficient nanocatalyst in C–O and C—C coupling reactions.

2. Experimental

2.1. Preparation of $MgFe_2O_4$@SiO_2@CBCE-Pd

For the synthesis of $MgFe_2O_4$@SiO_2@CBCE-Pd MNPs, first $MgFe_2O_4$@SiO_2 were synthesized by the co-precipitation method (Scheme 1) [27,28]. To synthesize the $MgFe_2O_4$@SiO_2@CBCE complex, 0.5 g of the prepared $MgFe_2O_4$@SiO_2 was dispersed in 35 mL EtOH by sonication for 20 min. Then, 1.5 mmol of 4′-Carboxybenzo-18-crown 6-Ether (CBCE) was added into the flask and stirred at reflux condition for 24 h. Once the reaction was completed, the $MgFe_2O_4$@SiO_2@CBCE product was separated using magnetic decantation, followed by thorough washing with EtOH and H_2O, and subsequently dried at 50 °C. Next, to prepare $MgFe_2O_4$@SiO_2@CBCE-Pd organometallic catalytic complex, a mixture of $MgFe_2O_4$@SiO_2@CBCE (0.5 g), Pd $(OAc)_2$ (1.5 mmol) and 30 ml EtOH was added into the flask and, then, it was stirred at 60 °C for 48 h under reflux conditions. The reaction vessel was finally treated with 2 mmol of $NaBH_4$ and stirred for a duration of 4 h. After the reaction was completed, the $MgFe_2O_4$@SiO_2@CBCE-Pd complex was separated, thoroughly washed with H2O and EtOH, and then dried in a vacuum at 50 °C.

2.2. Preparation of Suzuki reaction

A blend of aryl halides (1 mmol), phenylboronic acid (1.2 mmol), and potassium carbonate (1.4 mmol) was combined with 3 ml of water and the $MgFe_2O_4$@SiO_2@CBCE-Pd complex (0.03 g). The mixture was then stirred in open air at a temperature of 80 °C. The reaction's progress was monitored with TLC. Following that, the mixture underwent cooling and filtration. The samples were rinsed with water and then dried using 0.5 g of Sodium sulfate. Upon solvent removal, the desired products were achieved with outstanding yields as shown in Scheme 2.

2.3. General procedure for C–O reaction

A mixture of triphenyltin chloride (1.2 mmol), phenol (1 mmol), and K_2CO_3 (1.4 mmol) in the presence of $MgFe_2O_4$@SiO_2@CBCE-Pd (30 mg) was dissolved in MeOH and stirred at 60 °C. The progress of the reaction was checked by TLC technique in hexane solvent. Following the reaction, the $MgFe_2O_4$@SiO_2@CBCE-Pd was isolated using a magnet, then washed with ethyl acetate and H_2O, with sodium sulfate serving as a water absorbent. Subsequently, the organic solvent was evaporated to yield the pure products (Scheme 3).

2.4. Selected NMR data

1,1′-Biphenyl:^{1}H NMR (DMSO, 400 MHz): δ_H(ppm) = 7.15–7.41 (m, 10H).

4,4′-Dimethyl-1,1′-biphenyl:^{1}H NMR (DMSO, 400 MHz): δ_H(ppm) = 7.30–7.56 (m, 8H), 2.37 (s, 6H).

[1,1′-Biphenyl] −4-amine:^{1}H NMR (DMSO, 400 MHz): δ_H(ppm) = 7.25–7.43 (m, 8H), 4.91 (s, 2H).

4-Methoxy-4′-nitro-1,1′-biphenyl:^{1}H NMR (DMSO, 400 MHz): δ_H(ppm) = 6.99–8.14 (m, 8H), 4.09 (s, 3H).

2-Nitro-1,1′-biphenyl:^{1}H NMR (DMSO, 400 MHz): δ_H(ppm) = 7.18 (d, J = 8 Hz, 5H), 7.26–7.44 (m, 4H).

2-Methoxy-1,1′-biphenyl:^{1}H NMR (DMSO, 400 MHz): δ_H(ppm) = 7.34 (d, J = 12 Hz, 4H), 7.31 (s, 2H), 7.04 (s, 3H), 4.17 (s, 3H).

Oxydibenzene:^{1}H NMR (DMSO, 400 MHz): δ_H(ppm) = 7.46–7.78 (m, 10H).

2-Phenoxynaphthalene:^{1}H NMR (DMSO, 400 MHz): δ_H(ppm) = 7.24–7.89 (m, 12H).

1-Bromo-3-phenoxybenzene:^{1}H NMR (DMSO, 400 MHz): δ_H(ppm) = 7.20–7.65 (m, 9H).

1-Methyl-3-phenoxybenzene:^{1}H NMR (DMSO, 400 MHz): δ_H(ppm) = 7.13–7.75 (m, 9H), 1.21 (s, 3H).

Catalyst characterizations

The prepared $MgFe_2O_4$@SiO_2@CBCE-Pd MNPs were checked by SEM, ICP, XRD, FTIR, TGA, VSM, and EDS techniques.

The FTIR spectrum of each step of the synthesis of the desired catalyst was examined in the range of 400–4000 cm^{-1} in Fig. 1. The addition of each layer onto the previous one resulted in the emergence of distinct peaks representing new functional groups, providing evidence for the creation of a new layer. The absorption bands for $MgFe_2O_4$ (Fig. 1a) and $MgFe_2O_4$@SiO_2 (Fig. 1b) were in line with our previous findings, as reported. In Fig. 1c, two prominent bands at 2879 and 2961 cm^{-1} are observed, which are assigned to the aliphatic Carbon-e–Hydrogen stretching of amino acid CBCE. The presence of absorption bands at 1407 and 1659 cm^{-1} can be related to the C = C vibrations of the benzene ring, which confirm the successful binding of the organic ligand. The variation in the intensity of the $MgFe_2O_4$@SiO_2@CBCE-Pd peaks (Fig. 1d) provides crucial evidence confirming the coordination of the oxygen atom within the 4′-Carboxybenzo-18-crown 6-Ether (CBCE) to Palladium.

The crystalline structures of the $MgFe_2O_4$@SiO_2@CBCE-Pd were determined by XRD. Fig. 2 clearly demonstrates the highly crystalline cubic spinel structure of the obtained $MgFe_2O_4$, consistent with the standard $MgFe_2O_4$ XRD spectrum. The patterns reveal a crystallized arrangement specific to the (2 2 0), (3 1 1), (2 2 2), (4 0 0), (4 2 2), (5 1 1), and (4 4 0) crystallographic facets of magnetite. Furthermore, the XRD pattern of the nanocatalyst indicates that the $MgFe_2O_4$ phase remained unchanged following modifications with a different organic functional group (see Fig. 2). Fig. 2b shows the comparison of the XRD spectrum of the catalyst after recycling. As shown, there is no change in the XRD spectrum of the catalyst after recovery.

Thermal stability of TGA catalyst $MgFe_2O_4$@SiO_2@CBCE-Pd was investigated using TGA analysis. The slight decrease in weight (7 %) below 250 °C is caused by the elimination of absorbed solvents (see

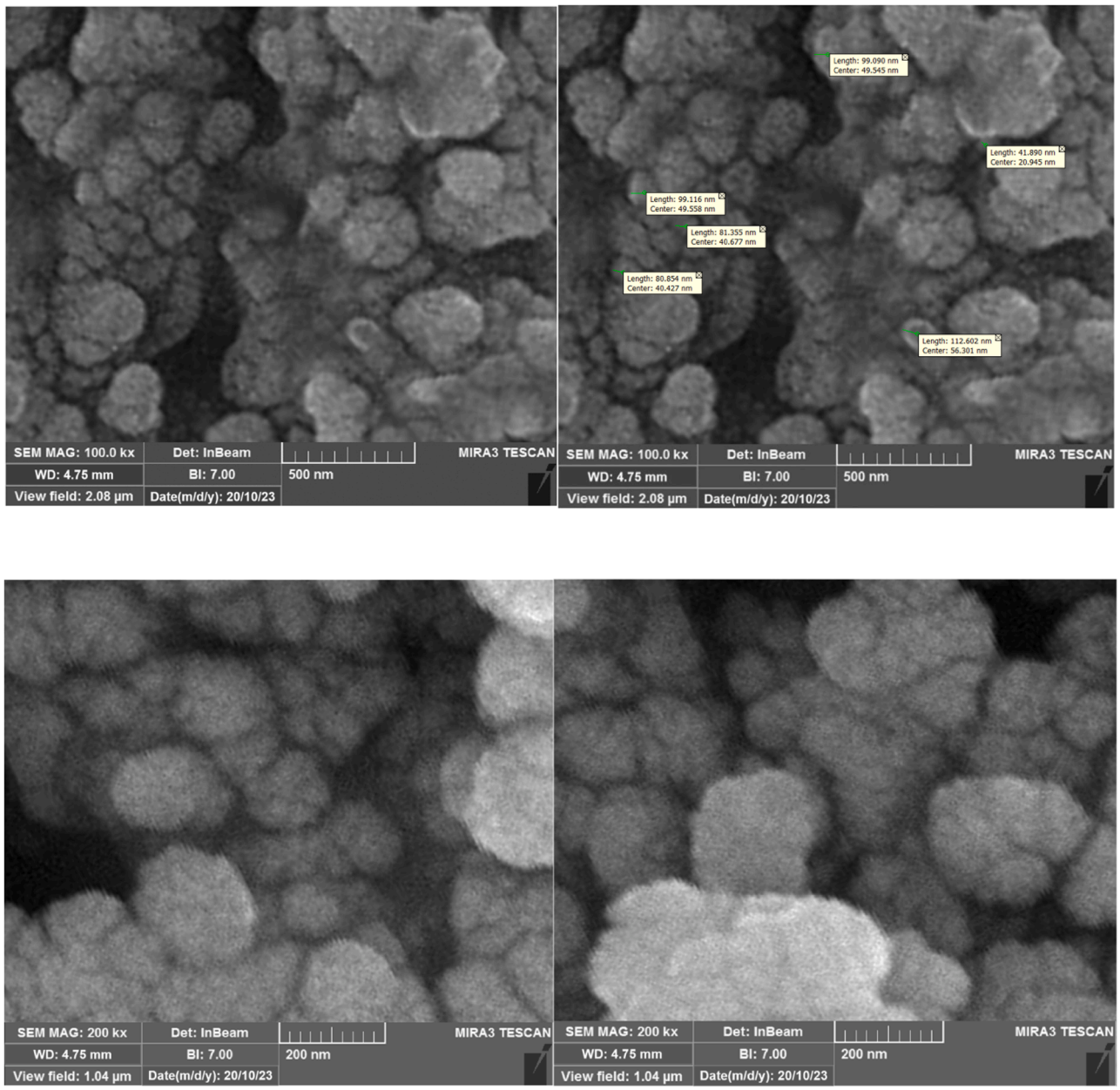

Fig. 5. SEM images of $MgFe_2O_4$@SiO_2@CBCE-Pd.

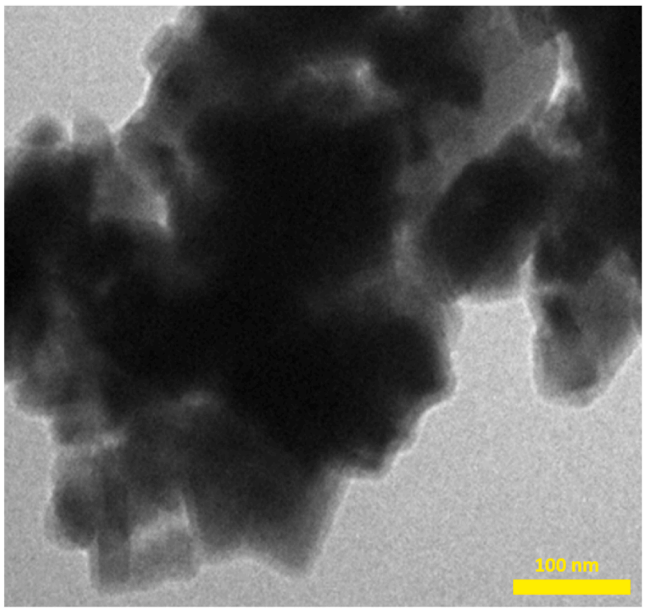

Fig. 6. TEM images of $MgFe_2O_4$@SiO_2@CBCE-Pd.

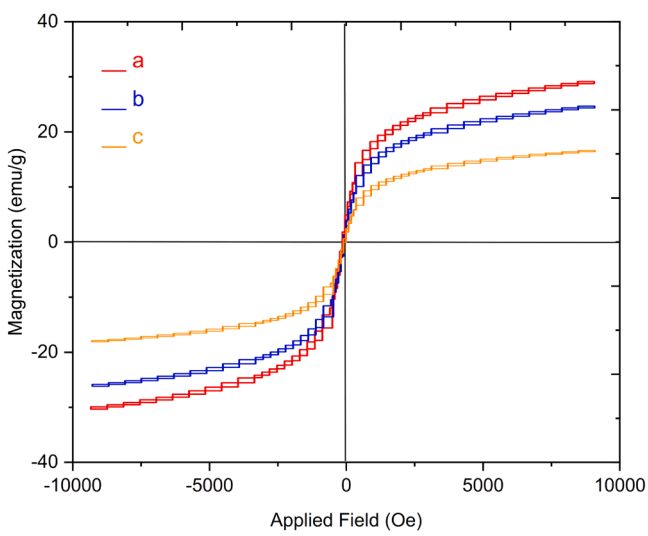

Fig. 7. VSM curves of (a) $MgFe_2O_4$(b) $MgFe_2O_4$@SiO_2 c) $MgFe_2O_4$@SiO_2@CBCE-Pd.

Fig. 3). Fig. 3 shows that the weight loss of 25 % between 200 and 800 °C for $MgFe_2O_4$@SiO_2@CBCE-Pd is attributed to the decomposition of the CBCE-Pd complex. The TGA curve results confirmed the successful support of CBCE-Pd on the surface of $MgFe_2O_4$ MNPs.

The EDX technique was used to analyze the elemental composition of $MgFe_2O_4$@SiO_2@CBCE-Pd. Furthermore, the EDX analysis affirmed the presence of all constituent elements (Mg, Fe, O, Si, Pd, and C) in the structure of $MgFe_2O_4$@SiO_2@CBCE-Pd (Fig. 4).

The SEM images of the $MgFe_2O_4$@SiO_2@CBCE-Pd samples (Fig. 5) validate the spherical structure of the prepared catalyst. The SEM image of $MgFe_2O_4$@SiO_2@CBCE-Pd confirms that the catalyst consists of uniformly-sized nanometer particles. Additionally, there are no significant changes in the surface morphology when the Palladium complex is introduced to $MgFe_2O_4$.

TEM was employed to provide additional insight into the morphology and loading of CBCE-Pd on the surface of $MgFe_2O_4$. A detailed examination of the TEM image verifies the formation of $MgFe_2O_4$@SiO_2@CBCE-Pd (Fig. 6).

Following that, the levels of palladium present in the initial catalyst and the palladium remaining after recycling the catalyst were examined using ICP analysis. The analysis revealed that the quantities of Pd in the new and recycled catalysts are 2.0×10^{-4} mol. g-1 and 1.9×10^{-4} mol. g^{-1} respectively, indicating minimal leaching of Pd from the $MgFe_2O_4$@SiO_2@CBCE-Pd framework.

The magnetic properties of $MgFe_2O_4$, $MgFe_2O_4$@SiO_2, and $MgFe_2O_4$@SiO_2@CBCE-Pd were analyzed using VSM techniques (Fig. 7). As anticipated, the reduction in saturation magnetization from approximately 30 and 26 emu/g to around 19 emu/g can be attributed to the presence of the newly coated layer, confirming the successful formation of the intended catalyst.

Catalytic studies

After investigating and identifying the structure of the nanocatalyst, the catalytic activity of $MgFe_2O_4$@SiO_2@CBCE-Pd was checked in the reactions of C—O and C—C pairs. At the beginning of our research, we examined the catalytic performance of $MgFe_2O_4$@SiO_2@CBCE-Pd in Suzuki coupling reactions. The model reaction chosen for this study involves the reaction between 1.2 mmol of phenylboronic acid and 1 mmol of iodobenzene using K_2CO_3 as a base at 80 °C. Various parameters including the amount of nanocatalyst, solvent, temperature, and base were investigated for this model reaction (see Table 1). Based on the findings, it can be inferred that the optimal conditions for this reaction entail the utilization of $MgFe_2O_4$@SiO_2@CBCE-Pd (0.03 g) and K_2CO_3 (1.4 mmol) as the base in H_2O at 80 °C.

After obtaining the optimized reaction conditions, we delved into examining the functional group tolerance of the established catalytic system ($MgFe_2O_4$@SiO_2@CBCE-Pd). In Table 2, it is evident that phenylboronic acid has the capability to react with various substrates containing electron-withdrawing or electron-donating substituents, resulting in the formation of corresponding products with high conversions of up to 99 %. The reaction proved effective when faced with a diverse range of functional groups on the Ar-Cl, Br, and I, resulting in outstanding conversion to the respective products. Various aryl bromides were subsequently treated with phenylboronic acid at specific intervals, yielding the intended biphenyl compounds as indicated in Table 2.

In Scheme 4, a possible mechanism for the Suzuki reaction in the presence of $MgFe_2O_4$@SiO_2@CBCE-Pd is demonstrated. During the Suzuki coupling process, the aryl halide undergoes an oxidative addition reaction with Pd. Subsequently, the reaction's base, potassium carbonate, activates phenylboronic acid to yield an ester derivative, phenyl boronate. This activated borane group then participates in a displacement reaction with the metal from medium (1) to generate medium (2). The final stage of this reaction involves an elimination-reduction process, resulting in the production of the desired product and the regeneration of the initial catalyst (Scheme 4).

After the preparation and characterization of $MgFe_2O_4$@SiO_2@CBCE-Pd, its catalytic activities were investigated in the C—O bond formation by triphenyltin chloride. Initially, we examined the reaction of Ph_3SnCl with phenol in different bases, solvents, and various amounts of $MgFe_2O_4$@SiO_2@CBCE-Pd (Table 3). The impact of varying amounts of nanocatalyst on the model reaction was investigated in MeOH as the solvent with triphenyl tin chloride at 60 °C in the absence of a catalyst. After a day, the intended biphenyl product was not achieved. Moreover, altering the documented catalyst amount significantly impacted the reaction's efficiency. The use of 0.03 g of $MgFe_2O_4$@SiO_2@CBCE-Pd was chosen as the optimal amount. Using H_2O, Acetonitrile, MeOH, EtOAc, or EtOH as the solvent also yielded the desired product in high amounts ranging from 35 % to 98 %. However, MeOH proved to be the most optimal choice. The optimal conditions for this reaction are $MgFe_2O_4$@SiO_2@CBCE-Pd catalyst (30 mg), phenol (1 mmol), triphenyltin chloride (1.2 mmol), and K_2CO_3 (1.4 mmol) as the base in the MeOH at 60 °C.

Table 1
Optimization of the model reaction of iodobenzene with phenylboronic acid catalyzed by $MgFe_2O_4@SiO_2@CBCE$-Pd.

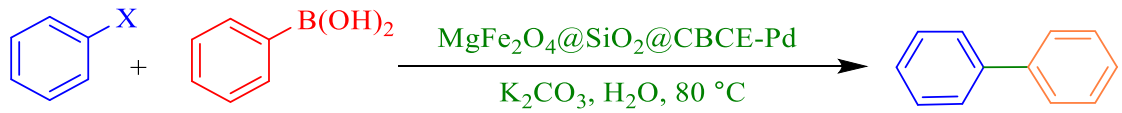

Entry	Nanocatalyst (g)	Solvent	Base	Temperature (°C)	Time (min)	Yield (%)[a]
1	–	H_2O	K_2CO_3	80	1 days	NR
2	0.007	H_2O	K_2CO_3	80	30	45
3	0.01	H_2O	K_2CO_3	80	30	75
4	0.02	H_2O	K_2CO_3	80	30	93
5	0.03	H_2O	K_2CO_3	80	30	99
6	0.04	H_2O	K_2CO_3	80	30	99
7	0.03	PEG-400	K_2CO_3	80	30	66
8	0.03	EtOH	K_2CO_3	80	30	82
9	0.03	MeOH	K_2CO_3	80	30	92
10	0.03	H_2O	Li_2CO_3	80	30	90
11	0.03	H_2O	*t*-BuOK	80	30	86
12	0.03	H_2O	NaOH	80	30	91
13	0.03	H_2O	Cs_2CO_3	80	30	85
14	0.03	H_2O	KOH	80	30	47
15	0.03	H_2O	$NaHCO_3$	80	30	40

[a] Isolated yield.

Table 2
Synthesis of Suzuki reaction from aryl halides using $MgFe_2O_4@SiO_2@CBCE$-Pd.

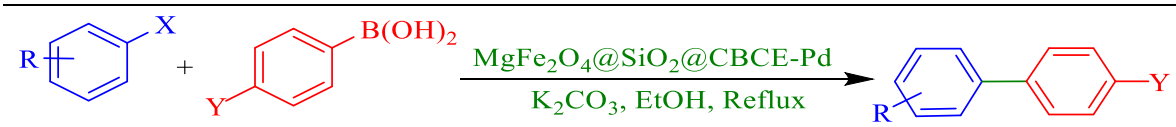

Entry	Y	X	R	Time (min)	Yield (%)[a]	TON	TOF (min^{-1})
1	H	I	H	30	99	165	330
2	H	I	4-Me	30	91	151	302
3	H	I	4-OMe	30	93	155	310
4	H	I	2-Me	50	95	158	197
5	4-OMe	I	H	120	89	148	74
6	H	I	4-COMe	60	85	141	141
7	H	I	4-OH	45	91	151	201
8	H	I	2-OMe	60	88	146	146
9	H	I	2-NO_2	60	90	150	150
10	H	I	5-Bromo-3-pyridine carboxaldehyde	120	–	–	–
11	H	Br	H	20	95	158	526
12	H	Br	4-NO_2	30	90	150	300
13	H	Br	4-Me	45	91	151	201
14	H	Br	4-OH	60	90	150	150
15	4-OMe	Br	4-NO_2	35	96	160	275
16	4-Me	Br	4-Me	60	93	155	155
17	H	Cl	H	60	91	151	151
18	4-OMe	Cl	4-NO_2	60	95	158	158
19	4-Me	Cl	H	40	90	150	250
20	H	Cl	4-OH	70	85	141	128
21	H	Cl	4-NH_2	60	93	155	155
22	H	Cl	4-Me	45	90	150	200

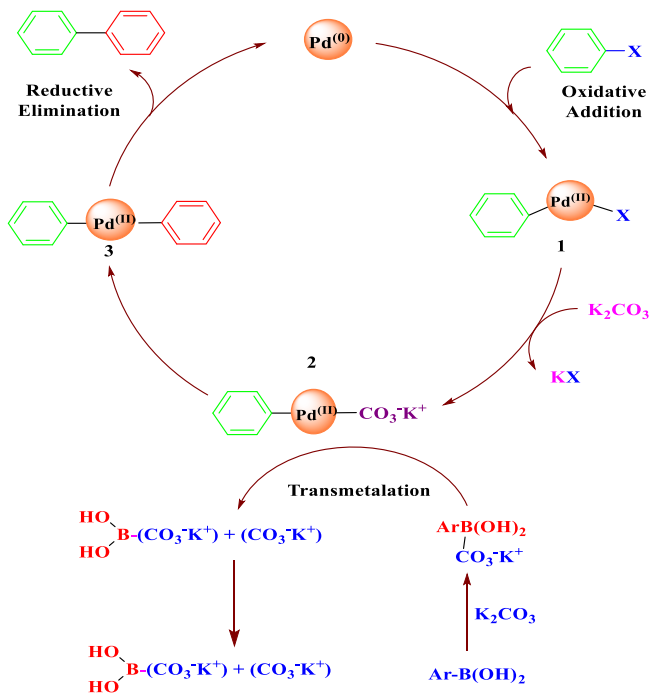

Scheme 4. Possible mechanism for Suzuki reaction.

After optimizing the reaction conditions, the Carbon-Oxcigen coupling reaction of various phenols with triphenyltin chloride (Ph_3SnCl) was tested (Table 4). Several phenols were studied in the coupling reaction with Ph_3SnCl in the presence of $MgFe_2O_4$@-SiO_2@CBCE-Pd. Both electron-rich and electron-deficient phenols successfully underwent C–O coupling reactions under gentle conditions. The desired products were obtained with 75 to 98 % efficiency.

The suggested process for the Carbon-Oxygen cross-coupling reaction, as depicted in Scheme 5 according to prior studies, unfolds as follows: Ph_3SnCl undergoes oxidative addition with Pd to generate intermediate (1). Subsequently, intermediate (1) engages with phenol to yield intermediate (2), and ultimately, via reductive elimination, intermediate (2) produces ether while liberating the Palladium nanoparticle.

3. Reusability of $MgFe_2O_4$@SiO_2@CBCE-Pd

In a separate experiment, the recyclability of the magnetic nanocatalyst was studied by examining the reaction between iodobenzene and phenylboronic acid as a model reaction in H_2O, employing 0.03 g of $MgFe_2O_4$@SiO_2@CBCE-Pd. The nanocatalyst, once synthesized, was separated using an external magnet and then thoroughly washed with ethyl acetate and H_2O multiple times. The reported catalyst was reused in four cycles without significant decrease in activity (Fig. 8).

Hot filtration test

To examine the palladium leaching phenomenon and the catalyst's heterogeneity during the process, a hot filtration test was performed for the iodobenzene-phenylboronic acid coupling reaction. The initial experiment resulted in a 66 % product yield at the midpoint of the reaction time (15 min). Subsequently, the reaction was replicated, and at the halfway point, the catalyst was removed, allowing the filtrate to continue reacting for an additional 15 min. At the 30-minute mark, the yield was determined to be 67 %, indicating the insignificance of palladium leaching in the reaction mixture.

Then, we showcased the effectiveness of $MgFe_2O_4$@SiO_2@CBCE-Pd by comparing the outcomes of the C—O and C–C cross-coupling reactions with those previously documented in the literature. When compared to other catalysts used in the synthesis of diphenyl ether and biphenyl, $MgFe_2O_4$@SiO_2@CBCE-Pd showed notably higher catalytic activity regarding both reaction time and yield (Table 5).

4. Conclusion

This study presents the development of an efficient method for producing $MgFe_2O_4$@SiO_2@CBCE-Pd, a novel, environmentally friendly, and recoverable catalyst. The characterization of the prepared $MgFe_2O_4$@SiO_2@CBCE-Pd catalyst was conducted using FT-IR, VSM, SEM, EDS, TEM, TGA, and XRD techniques. The new nanocatalyst was

Table 3
Enhancing various parameters for the phenol reaction with Ph_3SnCl.

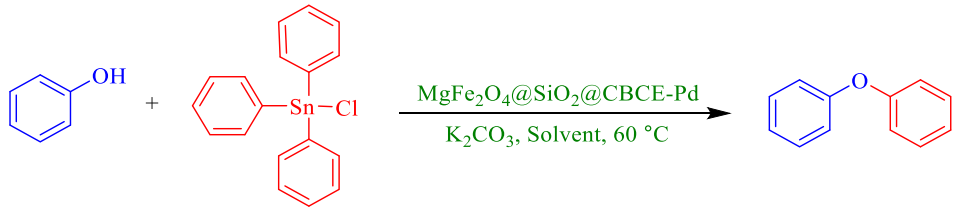

Entry	Catalyst (g)	Solvent	Base	Temperature (°C)	Time (h)	Yield (%)[a]
1	–	MeOH	K_2CO_3	60	1 days	N. R
2	0.008	MeOH	K_2CO_3	60	1.5	46
3	0.01	MeOH	K_2CO_3	60	1.5	73
4	0.02	MeOH	K_2CO_3	60	1.5	90
5	0.03	MeOH	K_2CO_3	60	1.5	98
6	0.04	MeOH	K_2CO_3	60	1.5	98
7	0.03	H_2O	K_2CO_3	60	1.5	40
8	0.03	EtOAc	K_2CO_3	60	1.5	75
9	0.03	Acetonitrile	K_2CO_3	60	1.5	82
10	0.03	EtOH	K_2CO_3	60	1.5	89
11	0.03	MeOH	Li_2CO_3	60	1.5	90
12	0.03	MeOH	Na_2CO_3	60	1.5	90
13	0.03	MeOH	Cs_2CO_3	60	1.5	88
14	0.03	MeOH	$NaHCO_3$	60	1.5	75
15	0.03	MeOH	KOH	60	1.5	45

[a] Isolated yield.

Table 4
At room temperature, phenol derivatives undergo a reaction with Ph_3SnCl.

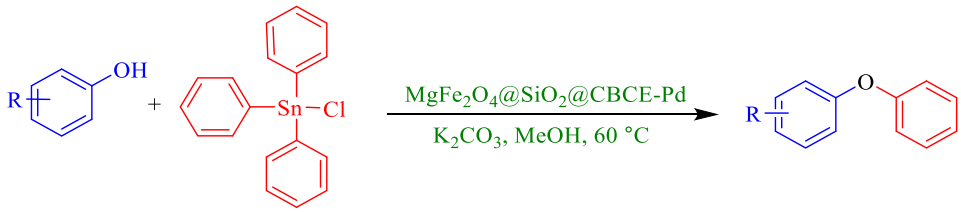

Entry	Ar	Product	Time (h)	Yield (%)[a]	TON	TOF (min^{-1})
1	Ph	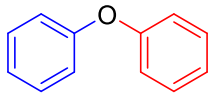	1.5	98	163	108
2	4-MePh	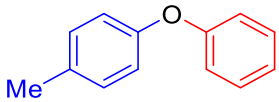	3	90	150	50
3	3-MePh	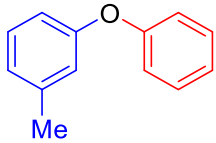	2.5	92	153	61
4	4-MeOPh	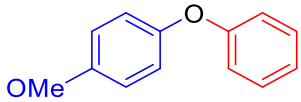	3	94	156	52
5	3-MeOPh	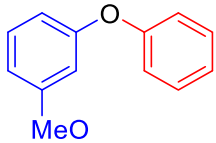	3	93	155	51
6	4-BrPh		3.5	89	148	42
7	3-BrPh	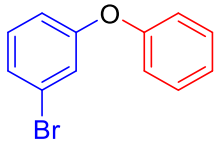	4	94	156	23
8	4-ClPh		2	96	160	80
9	4-NO_2Ph	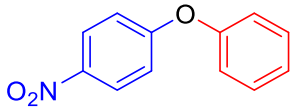	1.5	90	150	100
10	1-Naph	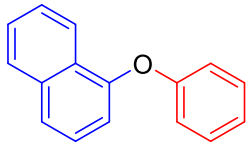	5	88	146	29
11	2-Naph	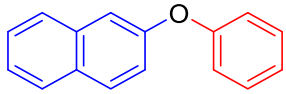	5	91	151	30

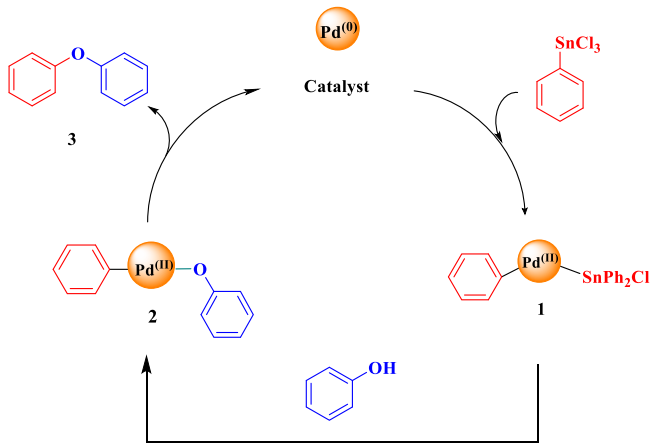

Scheme 5. Proposed mechanism for C–O coupling.

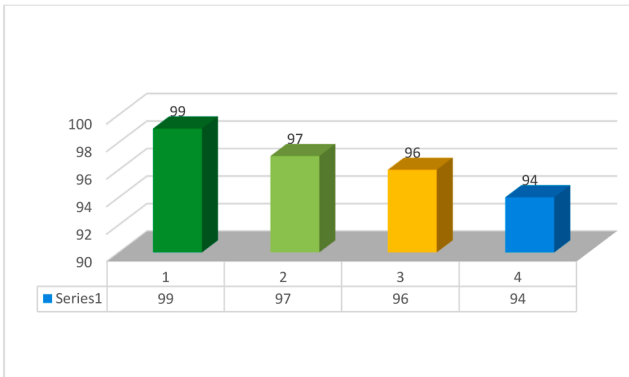

Fig. 8. Recyclability of $MgFe_2O_4$@SiO_2@CBCE-Pd in the synthesis of Suzuki (Series 1) reaction.

applied in the synthesis of C–O and C—C coupling reactions, demonstrating its effectiveness across a wide range of aryl halides such as Br, Cl, and Iodine. Importantly, this new $MgFe_2O_4$@SiO_2@CBCE-Pd catalyst can be easily produced from readily available materials. It was found that the reported catalyst can be reused four times without significant loss of activity or palladium metal leaching.

Funding information

The authors present their appreciation to King Saud University for funding this research through Researchers Supporting Program number (RSPD2024R779), King Saud University, Riyadh, Saudi Arabia.

CRediT authorship contribution statement

Durgesh Singh: Writing – original draft, Software, Resources, Project administration, Funding acquisition. **Anjan Kumar:** Project administration, Methodology, Investigation. **Yashwantsinh Jadeja:** Writing – review & editing, Project administration, Methodology, Investigation. **Soumya V Menon:** Writing – original draft, Visualization, Resources. **Priyanka Singh:** Writing – original draft, Supervision, Software, Resources. **Safaa Mohammed Ibrahim:** Software, Project administration, Methodology, Data curation. **Manmeet Singh:** Writing – original draft, Validation, Resources, Project administration, Methodology. **Munther Kadhim Abosaoda:** Resources, Project administration, Data curation. **Salwa Bader AlReshaidan:** Methodology, Investigation, Data curation. **Mohammed A. El-Meligy:** Resources, Project administration, Methodology, Investigation.

Declaration of competing interest

The authors affirm that they do not have any known competing financial interests or personal relationships that could have seemed to influence the work reported in this paper.

Data availability

No data was used for the research described in the article.

Table 5
Assessing the catalytic activity of $MgFe_2O_4$@SiO_2@CBCE-Pd in the C–C coupling reaction compared to previously documented methods.

Entry	Nanocatalyst	Ar-X	Product	Time (min)	Yield (%)	Ref.
1	Pd/SH-SiO_2	Ar-I	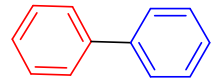	12h	95	[29]
2	Pd@MTiO_2	Ar-I		180	99	[30]
3	CA/Pd (0)	Ar-I		120	94	[31]
4	PANI-Pd	Ar-I		240	91	[32]
5	$MgFe_2O_4$@SiO_2@CBCE-Pd	Ar-I		30	99	This work
6	$Cu(OAc)_2$	Ar-OH	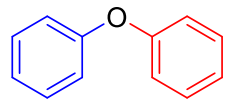	30h	80	[33]
7	MCM-41-Biurea-Pd	Ar-OH	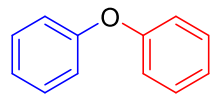	19h	92	[34]
8	$MgFe_2O_4$@SiO_2@CBCE-Pd	Ar-OH	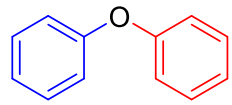	1.5 h	98	This work

Supplementary materials

Supplementary material associated with this article can be found, in the online version, at doi:10.1016/j.molstruc.2024.140133.

References

[1] M.A. Ashraf, Z. Liu, C. Li, D. Zhang, Fe3O4@HcdMeen-Pd(0) Organic–Inorganic Hybrid: as a Novel Heterogeneous Nanocatalyst for Chemo and Homoselective Heck C–C Cross-Coupling Synthesis of Butyl Cinnamates, Catal. Lett. (2021), https://doi.org/10.1007/s10562-020-03509-0.

[2] H. Zhao, et al., In vitro toxicity evaluation of ultra-small MFe2O4 (M = Fe, Mn, Co) nanoparticles using A549 cells, RSC Adv. 5 (2015) 68454–68460.

[3] A.M. Demin, A.V. Vakhrushev, A.V. Mekhaev, M.A. Uimin, V.P. Krasnov, Modification of Fe3O4 magnetic nanoparticles with a GRGD peptide, Russ. Chem. Bull. 70 (2021) 449–456.

[4] A. Taheri Kal Koshvandi, M.M. Heravi, T. Momeni, Current Applications of Suzuki–Miyaura Coupling Reaction in The Total Synthesis of Natural Products: an update, Appl. Organomet. Chem. 32 (2018) e4210.

[5] Z. Chen, et al., A heterogeneous single-atom palladium catalyst surpassing homogeneous systems for Suzuki coupling, Nat. Nanotechnol. 13 (2018) 702–707.

[6] M.A. Ashraf, Z. Liu, D. Zhang, A. Alimoradi, L-lysine-Pd Complex Supported on Fe 3 O 4 MNPs: a novel recoverable magnetic nanocatalyst for Suzuki C-C Cross-Coupling reaction, Appl. Organomet. Chem. 34 (2020) e5668.

[7] J. Lakshmidevi, B.R. Naidu, K. Venkateswarlu, CuI in biorenewable basic medium: three novel and low E-factor Suzuki-Miyaura cross-coupling reactions, Molecul. Cataly. 522 (2022) 112237.

[8] S. Gorji, R. Ghorbani-Vaghei, Ag nanoparticles stabilized on basalt fibers as a novel, stable, and reusable catalyst for Suzuki–Miyaura coupling reactions, Appl. Organomet. Chem. 35 (2021).

[9] H. Azizollahi, H. Eshghi, J.-A. García-López, Fe3O4-SAHPG-Pd0 nanoparticles: a ligand-free and low Pd loading quasiheterogeneous catalyst active for mild Suzuki–Miyaura coupling and C-H activation of pyrimidine cores, Appl. Organomet. Chem. 35 (2021).

[10] Y. Lei, W. Zhu, Y. Wan, R. Wang, H. Liu, Pd nanoparticles supported on amphiphilic porous organic polymer as an efficient catalyst for aqueous hydrodechlorination and Suzuki-Miyaura coupling reactions, Appl. Organomet. Chem. 34 (2020).

[11] J. Chen, J. Zhang, Y. Zhang, M. Xie, T. Li, Nanoporous phenanthroline polymer locked Pd as highly efficient catalyst for Suzuki-Miyaura Coupling reaction at room temperature, Appl. Organomet. Chem. 34 (2020).

[12] S.R. Aabaka, et al., Nanocellulose Supported PdNPs as in situ Formed Nano Catalyst for the Suzuki Coupling Reaction in Aqueous Media: a Green Approach and Waste to Wealth, J. Organomet. Chem. 937 (2021) 121719.

[13] C. Han, et al., Enhanced support effects in single-atom copper-incorporated carbon nitride for photocatalytic suzuki cross-coupling reactions, Appl. Cataly. B: Environ. 320 (2023) 121954.

[14] C.-J. Li, Reflection and perspective on green chemistry development for chemical synthesis - Daoist insights, Green Chem. 18 (2016) 1836–1838.

[15] C.C.C. Johansson Seechurn, M.O. Kitching, T.J. Colacot, V Snieckus, Palladium-catalyzed cross-coupling: a historical contextual perspective to the 2010 nobel prize, Angewand. Chem. - Int. Editi. 51 (2012) 5062–5085.

[16] N. Muniyappan, S. Sabiah, Synthesis, structure, and characterization of picolyl- and benzyl-linked biphenyl palladium N-heterocyclic carbene complexes and their catalytic activity in acylative cross-coupling reactions, Appl. Organomet. Chem. 34 (2020).

[17] H. Alamgholiloo, S. Rostamnia, N. Noroozi Pesyan, Extended architectures constructed of thiourea-modified SBA-15 nanoreactor: a versatile new support for the fabrication of palladium pre-catalyst, Appl. Organomet. Chem. 34 (2020).

[18] H. Sun, D. Li, Recyclable MFe2O4(M = Mn, Zn, Cu, Ni, Co) coupled micro-nano bubbles for simultaneous catalytic oxidation to remove NO: X and SO2in flue gas, RSC Adv. 10 (2020) 25155–25164.

[19] K. Wang, P. Yang, R. Guo, X. Yao, W. Yang, Photothermal performance of MFe2O4 nanoparticles, Chin. Chem. Lett. 30 (2019) 2013–2016.

[20] Dippong, T. & Levei, E.A. Chapter III Synthesis and characterization of MFe 2 O 4 (M : zn, Ca, Mg) photocatalysts. 4, 1–12 (2021).

[21] C. Singh, Devika, R. Malik, V. Kumar, S Singhal, CdS nanorod-MFe2O4 (M = Zn, Co and Ni) nanocomposites: a heterojunction synthesis strategy to mitigate environmental deterioration, RSC Adv. 5 (2015) 89327–89337.

[22] I. Ibrahim, I.O. Ali, T.M. Salama, A.A. Bahgat, M.M. Mohamed, Synthesis of magnetically recyclable spinel ferrite (MFe2O4, M=Zn, Co, Mn) nanocrystals engineered by sol gel-hydrothermal technology: high catalytic performances for nitroarenes reduction, Appl. Cataly. B: Environ. 181 (2016) 389–402.

[23] S. Zhang, et al., Study on the construction of char-supported NiFe-NiFe2O4 catalyst and its catalytic cracking mechanism of biomass tar under relative low temperature, Fuel 346 (2023) 128412.

[24] D. Yim, et al., Ultrathin WO3 Nanosheets Converted from Metallic WS2 Sheets by Spontaneous Formation and Deposition of PdO Nanoclusters for Visible Light-Driven C-C Coupling Reactions, ACS Appl. Mater. Interface. 11 (2019) 36960.

[25] A. Liu, et al., Erratum: intensified energy storage in high-voltage nanohybrid supercapacitors via the efficient coupling between TiNb2O7/Holey-rGO nanoarchitectures and ionic liquid-based electrolytes (ACS Appl. Mater. Interfaces (2021) 13:18 (21349-21361) DOI: 10.1021/, ACS Appl. Mater. Interface. 13 (2021) 37937–37938.
[26] Q. Gu, Q. Jia, J. Long, Z. Gao, Heterogeneous Photocatalyzed C–C Cross-coupling Reactions Under Visible-light and Near-infrared Light Irradiation, ChemCatChem 11 (2019) 669.
[27] F. Zhang, B. Shen, W. Jiang, H. Yuan, H. Zhou, Hydrolysis extraction of diosgenin from Dioscorea nipponica Makino by sulfonated magnetic solid composites, J. Nanopart. Res. 21 (2019).
[28] I. Dindarloo Inaloo, S. Majnooni, H. Eslahi, M. Esmaeilpour, N-Arylation of (hetero)arylamines using aryl sulfamates and carbamates via C–O bond activation enabled by a reusable and durable nickel(0) catalyst, New J. Chem. 44 (2020) 13266–13278.
[29] K. Gude, R. Narayanan, Synthesis and characterization of colloidal-supported metal nanoparticles as potential intermediate nanocatalysts, J. Phys. Chem. C 114 (2010) 6356–6362.
[30] P. Mondal, et al., Palladium nanoparticles embedded on mesoporous TiO2 material (Pd@MTiO2) as an efficient heterogeneous catalyst for Suzuki-Coupling reactions in water medium, J. Colloid Interface. Sci. 508 (2017) 378–386.
[31] V.W. Faria, et al., Palladium nanoparticles supported in a polymeric membrane: an efficient phosphine-free "green" catalyst for Suzuki–Miyaura reactions in water, RSC Adv. 4 (2014) 13446–13452.
[32] H.A. Patel, A.L. Patel, A.V. Bedekar, Polyaniline-anchored palladium catalyst-mediated Mizoroki–Heck and Suzuki–Miyaura reactions and one-pot Wittig–Heck and Wittig–Suzuki reactions, Appl. Organomet. Chem. 29 (2015) 1–6.
[33] N. Iranpoor, H. Firouzabadi, E. Etemadi Davan, A. Rostami, A. Nematollahi, Triphenyltin chloride as a new source of phenyl group for C-heteroatom and C–C bond formation, J. Organomet. Chem. 740 (2013) 123–130.
[34] H. Batmani, N. Noroozi Pesyan, F. Havasi, Synthesis and characterization of MCM-41-Biurea-Pd as a heterogeneous nanocatalyst and using its catalytic efficacy in C–C, C–N and C–O coupling reactions, Appl. Organomet. Chem. 32 (2018) e4419.